



Influences of the separation distance, ship speed and channel dimension on ship maneuverability in a confined waterway

Peng Du ^{a,*}, Abdellatif Ouahsine ^{a,*}, Philippe Sergent ^b

^a Laboratoire Roberval, UMR-CNRS 7337, Sorbonne Universités, Université de technologie de Compiègne, Centre de recherches de Royallieu, CS 60319, 60203 Compiègne cedex, France

^b Cerema, 134, rue de Beauvais, CS 60039, 60200 Compiègne cedex, France

ARTICLE INFO

Article history:

Received 15 October 2017

Accepted 31 January 2018

Available online 14 February 2018

Keywords:

Ship maneuvering

Confined waterway

Bank effect

Trajectory

System-based method

Turning circle test

ABSTRACT

Ship maneuvering in the confined inland waterway is investigated using the system-based method, where a nonlinear transient hydrodynamic model is adopted and confinement models are implemented to account for the influence of the channel bank and bottom. The maneuvering model is validated using the turning circle test, and the confinement model is validated using the experimental data. The separation distance, ship speed, and channel width are then varied to investigate their influences on ship maneuverability. With smaller separation distances and higher speeds near the bank, the ship's trajectory deviates more from the original course and the bow is repelled with a larger yaw angle, which increase the difficulty of maneuvering. Smaller channel widths induce higher advancing resistances on the ship. The minimum distance to the bank are extracted and studied. It is suggested to navigate the ship in the middle of the channel and with a reasonable speed in the restricted waterway.

© 2018 Académie des sciences. Published by Elsevier Masson SAS. This is an open access article under the CC BY-NC-ND license (<http://creativecommons.org/licenses/by-nc-nd/4.0/>).

1. Introduction

During the inland transport, ships will inevitably be maneuvered in restricted areas, where the hydrodynamic interactions are critical. When the ship moves near the bank, the bow will be pushed away by the bank, known as the bow cushion, and the body is attracted towards the bank, known as the bank suction. If these effects exceed a certain level, ships become difficult to control, which may lead to marine accidents like collision and grounding. It is therefore of great importance and significance to investigate ship maneuvering in restricted waters.

The study of ship maneuvering has a long history and is still developed today by researchers. By using captive model tests and some mathematical methods, hydrodynamic coefficients can be determined at the early stage. Then system-based simulation can be conducted to predict ship maneuverability. Compared with experimental and CFD (Computational Fluid Dynamics) methods, it only requires a few minutes for one free running trial on a PC (Personal Computer). This is very efficient during the preliminary evaluations in the design of the ship, and the results can be satisfactory as long as the models and coefficients are accurate enough. Artificial neural networks ([1,2]), support vector machines ([3]), and optimization techniques ([4,5]) have been used to identify the hydrodynamic derivatives of ships and to simulate ship maneuvering. With these techniques, ship parameters can be optimized and maneuvering simulations can be carried out with high precision.

* Corresponding authors.

E-mail addresses: pp1565156@126.com (P. Du), ouahsine@utc.fr (A. Ouahsine).

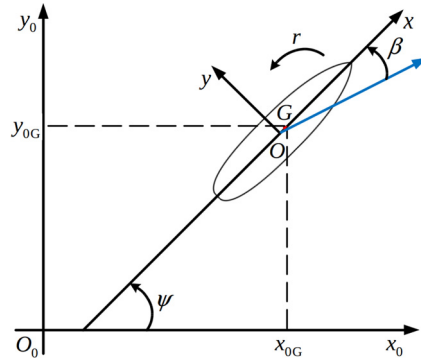


Fig. 1. Coordinate system for ship maneuvering analysis.

Several works have been conducted for ship maneuvering in restricted waters using the system-based method. Lee and Lee [6] investigated ship maneuvering with ship–bank interactions. It was found that when the ship approached a wedge-shaped bank, it might encounter a dangerous tendency of collision due to the combined effect of the attracting sway force and a bow-in moment. Another work of Lee [7] assessed the safe navigation between ships in restricted waterways. The smaller ship was found to be more influenced by ship–ship interactions, and appropriate safe speed and distance were proposed. With more advanced models, the precision of this method can be increased, and more practical results can be obtained.

In the present paper, ship maneuvering in the confined waterway is investigated using a system-based method. The influences of the channel bank and bottom are implemented as external forces in the nonlinear maneuvering equations. The separation distances, ship speeds, and channel dimensions are varied to investigate the confinement effect on the trajectories and yaw angles of the ship. The minimum distances between the ship and the bank are fitted as functions of these factors to quantitatively characterize ship navigation in restricted waterways.

2. Maneuvering equations

2.1. Nonlinear transient hydrodynamic model

As shown in Fig. 1, the maneuvering simulations in this study are conducted in 2D with three degrees of freedom (DOF). The origin of the body-fixed system is fixed at the midship point. The transient equations of motion under this coordinate system can be written as ([5]):

$$X = m (\dot{u} - vr - x_G r^2) \tag{1}$$

$$Y = m (\dot{v} + ur + x_G \dot{r}) \tag{2}$$

$$N = I_z \dot{r} + m x_G (\dot{v} + ur) \tag{3}$$

where X, Y, N are the external forces and moment acting on the ship's hull. m is the mass of the ship. u and v are the surge and sway velocities respectively. $r = \dot{\psi}$ is the yaw rate. I_z is the moment of inertia about the z axis. (x_G, y_G) is the position of the gravity center. $y_G = 0$ since the ship is assumed to be symmetric. The Bis-system is used to non-dimensionalize equations (1)–(3).

$$\dot{u} - vr - x_G r^2 = gX'' \tag{4}$$

$$\dot{v} + ur + x_G \dot{r} = gY'' \tag{5}$$

$$L^2 k_z^2 \dot{r} + x_G (\dot{v} + ur) = gLN'' \tag{6}$$

where $k_z'' = \frac{1}{L} \sqrt{\frac{I_z}{m}}$ is the non-dimensional radius of gyration. X'', Y'' and N'' are the non-dimensional forces and moment.

The Esso Bernicia 190,000 DWT tanker is selected for the maneuvering analysis in this study, whose parameters can be seen in Table 1. By adopting the Taylor expansions and maintaining only the most significant parameters, the following nonlinear hydrodynamic equations can be obtained:

$$\begin{aligned} gX'' = & X''_{\dot{u}} \dot{u} + \frac{1}{L} X''_{|u|u} u |u| + X''_{vr} vr + \frac{1}{L} X''_{|v|v} v |v| \\ & + \frac{1}{L} X''_{c|c|\delta\delta} c |c| \delta^2 + \frac{1}{L} X''_{c|c|\beta\delta} c |c| \beta \delta + gT''_p (1 - t_d) \\ & + X''_{\dot{u}\xi} \dot{u}\xi + \frac{1}{L} X''_{|u|\xi} |u| u\xi + X''_{vr\xi} vr\xi + \frac{1}{L} X''_{v\xi\xi} v^2 \xi^2 \end{aligned} \tag{7}$$

Table 1
Geometrical parameters of the Esso Bernicia 190,000 DWT tanker.

Geometrical parameters	Values
Length between perpendiculars (L_{pp})	304.8 [m]
Beam (B)	47.17 [m]
Draft to design waterline (T)	18.46 [m]
Displacement (∇)	220,000 [m ³]
L_{pp}/B	6.46
B/T	2.56
Block coefficient (C_B)	0.83
Design speed (u_0)	16 [knots]
Normal propeller (n)	80 [rpm]

Table 2
Hydrodynamic coefficients of the Esso Bernicia 190,000 DWT tanker.

No.	Coefficients	Values	No.	Coefficients	Values
1	$X''_{\dot{u}}$	-0.0500	18	$Y''_{ v v\zeta}$	-1.5000
2	X''_{vr}	1.0200	19	$N''_{vr\zeta}$	-0.1200
3	$Y''_{\dot{v}}$	-0.0200	20	$Y''_{ c c\delta}$	0.1794
4	$Y''_{ c c \beta \delta }$	-2.1600	21	$Y''_{uv\zeta}$	0.0000
5	Y''_T	0.0500	22	$N''_{uv\zeta}$	-0.2043
6	N''_T	-0.0200	23	$X''_{c c \beta\delta}$	0.1220
7	N''_r	-0.0608	24	$N''_{ c c\delta}$	-0.0883
8	$Y''_{ v v}$	-2.4000	25	$X''_{vv\zeta\zeta}$	0.0125
9	$N''_{ v r}$	-0.3000	26	$N''_{ c c \beta \delta }$	0.6880
10	$X''_{ v v}$	0.3000	27	$Y''_{ c c \beta \delta \zeta}$	-0.1910
11	Y''_{uv}	-1.2050	28	$N''_{ c c \beta \delta \zeta}$	0.3440
12	N''_{uv}	-0.4510	29	Y''_{ur}	0.2480
13	$X''_{\dot{u}\zeta}$	-0.0500	30	N''_{ur}	-0.1717
14	$Y''_{\dot{v}\zeta}$	-0.3780	31	$X''_{u u }$	-0.0312
15	$Y''_{ur\zeta}$	0.1420	32	$N''_{r\zeta}$	-0.0054
16	$N''_{ur\zeta}$	-0.0448	33	$X''_{ u u\zeta}$	-0.0050
17	$X''_{vr\zeta}$	0.3780	34	$X''_{c c \delta\delta}$	-0.0984

$$\begin{aligned}
 gY'' &= Y''_{\dot{v}}\dot{v} + \frac{1}{L}Y''_{uv}uv + \frac{1}{L}Y''_{|v|v}|v|v + \frac{1}{L}Y''_{|c|c\delta}|c|c\delta + Y''_{ur}ur \\
 &\quad + \frac{1}{L}Y''_{|c|c|\beta|\delta|}|c|c|\beta|\beta|\delta| + Y''_TgT_p + Y''_{ur\xi}ur\xi + \frac{1}{L}Y''_{uv\xi}uv\xi \\
 &\quad + Y''_{\dot{v}\xi}\dot{v}\xi + \frac{1}{L}Y''_{|v|v\xi}|v|v\xi + \frac{1}{L}Y''_{|c|c|\beta|\delta|\xi}|c|c|\beta|\beta|\delta|\xi
 \end{aligned} \tag{8}$$

$$\begin{aligned}
 gLN'' &= L^2N''_r\dot{r} + N''_{uv}uv + LN''_{|v|r}|v|r + N''_{|c|c\delta}|c|c\delta + LN''_{ur}ur \\
 &\quad + N''_{|c|c|\beta|\delta|}|c|c|\beta|\beta|\delta| + N''_TgT_p + LN''_{ur\xi}ur\xi + L^2N''_{r\xi}\dot{r}\xi \\
 &\quad + N''_{uv\xi}uv\xi + LN''_{|v|r\xi}|v|r\xi + N''_{|c|c|\beta|\delta|\xi}|c|c|\beta|\beta|\delta|\xi
 \end{aligned} \tag{9}$$

where $X''_{\dot{u}}, X''_{u|u|}, \dots$ are the non-dimensional hydrodynamic derivatives. The optimized ones in [8] are used in this work, whose values are shown in Table 2. g, δ, t_d and β are the gravitational acceleration, rudder angle, thrust deduction coefficient and drift angle. $\xi = T/(h - T)$, where h and T are the water depth and ship draft. The non-dimensional propeller thrust T''_p and the flow velocity at the rudder c are given by:

$$T''_p = \frac{1}{gL}T''_{uu}u^2 + \frac{1}{g}T''_{un}un + \frac{L}{g}T''_{|n|n}|n|n \tag{10}$$

$$c^2 = c_{un}un + c_{nn}n^2 \tag{11}$$

where T_{uu}, T_{un} and $T_{|n|n}$ are the hydrodynamic coefficients of the propeller. c_{un} and c_{nn} are the hydrodynamic coefficients of the rudder. n is the revolution rate. A relation between equations (4)–(6) and equations (7)–(9) can be established and the ship motion parameters $u, v, r, x, y, \psi, \delta, n$, etc. can then be solved.

2.2. Formulations of the confinement effect

The confinement effects are treated as external forces and moments acting on the ship’s hull, which can be directly included in the RHS (right-hand side) of equations (4)–(6). The model of [9] is adopted for their calculations, where they are decomposed as follows:

$$\begin{aligned} Y_B &= Y_B^H + Y_B^P + Y_B^{HP} \\ N_B &= N_B^H + N_B^P + N_B^{HP} \end{aligned} \tag{12}$$

where the superscript ‘H’ denotes the effect of the forward speed, ‘P’ denotes the effect of ship propulsion, ‘HP’ denotes the coupled effects of the forward speed and propulsion. The Vantorre’s model lacks the expression for the longitudinal force X_B , which will be introduced later. The terms in the RHS of equation (12) are written as:

$$Y_B^H = \frac{1}{2} \rho L T u^2 \sum_{i=1}^2 \sum_{k=0}^2 \alpha_{ik}^H y_B^i \left(\frac{T}{h_{\text{eff}} - T} \right)^k \tag{13}$$

$$N_B^H = \frac{1}{2} \rho L^2 T u^2 \sum_{i=1}^2 \sum_{k=0}^2 \beta_{ik}^H y_B^i \left(\frac{T}{h_{\text{eff}} - T} \right)^k \tag{14}$$

$$Y_B^P = \frac{1}{2} \rho L T V_T^2 \sum_{i=1}^2 \sum_{k=0}^2 \alpha_{ik}^P y_{B3}^i \left(\frac{T}{h_{\text{eff}} - T} \right)^k \tag{15}$$

$$N_B^P = \frac{1}{2} \rho L^2 T V_T^2 \sum_{i=1}^2 \sum_{k=0}^2 \beta_{ik}^P y_{B3}^i \left(\frac{T}{h_{\text{eff}} - T} \right)^k \tag{16}$$

$$Y_B^{HP} = \frac{1}{2} \rho L T V_T^2 F_r \sum_{i=1}^2 \sum_{k=0}^2 \alpha_{ik}^{HP} y_{B3}^i \left(\frac{T}{h_{\text{eff}} - T} \right)^k \tag{17}$$

$$N_B^{HP} = \frac{1}{2} \rho L^2 T V_T^2 F_r \sum_{i=1}^2 \sum_{k=0}^2 \beta_{ik}^{HP} y_{B3}^i \left(\frac{T}{h_{\text{eff}} - T} \right)^k \tag{18}$$

where ρ is the water density. $\alpha_{ik}^H, \beta_{ik}^H, \alpha_{ik}^P, \beta_{ik}^P, \alpha_{ik}^{HP}, \beta_{ik}^{HP}$ are the regression coefficients, which can be found in [8]. F_r is the Froude number based on the ship’s length. $h_{\text{eff}} = h - z_m$ is the effective depth of the channel, where h and z_m are the water depth and the average sinkage due to the squat effect. V_T is a reference velocity defined as:

$$V_T = \sqrt{\left| \frac{T_p}{\frac{1}{8} \rho \pi D^2} \right|} \tag{19}$$

where T_p is the propeller thrust. D is the propeller diameter. y_B and y_{B3} are the non-dimensional ship–bank distances defined as:

$$y_B = \frac{1}{2} B \left(\frac{1}{y_p} + \frac{1}{y_s} \right) \tag{20}$$

$$y_{B3} = \frac{1}{2} B \left(\frac{1}{y_{p3}} + \frac{1}{y_{s3}} \right) \tag{21}$$

The definitions of y_p, y_{p3}, y_s, y_{s3} are shown in Fig. 2. Note that the separation distance between ship and bank, i.e. the initial ship–bank distance on the starboard side, in the following studies refers to y_s . Some limitations have to be respected when using Vantorre’s model. The ship’s geometry should satisfy: $0.56 < C_B < 0.84, 6.0 < L/B < 7.3, h/T_d > 1.07$. And the testing conditions are better if they are within the range: $0 < Fr < 0.081, 0 < y_{B3} < 0.79$.

Regarding the longitudinal force, we adopt here the model of Lataire [10],

$$X_B = \alpha_X \rho g \nabla m_{\text{eq}}^2 T u_m(u) \tag{22}$$

where α_X is a regression coefficient from experiments. ∇ is the displacement of the ship. $T u_m(u)$ is an adapted Tuck number.

$$T u_m(u) = \frac{(Fr_h / Fr_{\text{crit}})^2}{\sqrt{1 - (Fr_h / Fr_{\text{crit}})^2}} \tag{23}$$

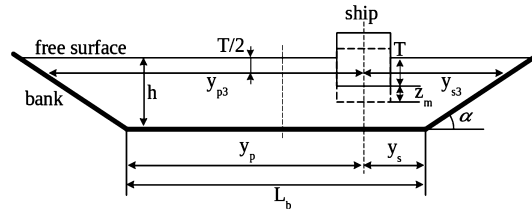


Fig. 2. Parameter definitions of a ship in the confined waterway (cross section).

Table 3

Ship parameters in the turning circle test. u_{init} is the initial surge velocity.

Parameters	Values
δ [°]	35
n [rpm]	80
u_{init} [knots]	10.30
T [m]	18.46
h [m]	25.5

$Fr_{crit} = (2 \sin(\arcsin(1 - m_b)/3))^{1.5}$ is the critical Froude number ([11,12]). Fr_h is the water depth-dependent Froude number. m_b and m_{eq} are the classic and equivalent blockages defined as:

$$m_b = \frac{A_{ship}}{A_{channel}} \quad m_{eq} = \frac{\chi_{ship}}{\chi_s + \chi_p} - \frac{\chi_{ship}}{\chi_{channel}} \tag{24}$$

where A_{ship} and $A_{channel}$ are the midship area and the cross-section area of the channel. The weighting coefficients of the cross section χ can be calculated as:

$$\chi_s = \int_0^h \int_0^{y_s} e^{-(\alpha_y \frac{|y|}{y_d} + \alpha_z \frac{|z|}{T})} dy dz \tag{25}$$

$$\chi_p = \int_0^h \int_0^{y_p} e^{-(\alpha_y \frac{|y|}{y_d} + \alpha_z \frac{|z|}{T})} dy dz \tag{26}$$

$$\chi_{ship} = 2 \frac{y_d T}{\alpha_y \alpha_z} (1 - e^{-\frac{\alpha_y B}{2y_d}}) (1 - e^{-\alpha_z}) \tag{27}$$

$$\chi_{channel} = 2 \frac{y_d T}{\alpha_y \alpha_z} \tag{28}$$

where the subscripts 's' and 'p' represent the starboard and port sides of the ship. The definitions of the weighting coefficients can be found in detail in Fig. 3. A position closer to the ship corresponds to a larger confinement effect in the channel. α_y and α_z are the regression coefficients obtained from experiments. y_d is the influence distance which can be described as the boundary between open and confined waters, which can be calculated as:

$$y_d = B(5Fr_h + 5) \tag{29}$$

A ship sailing at a distance larger than y_d does not encounter significant bank effects. In this study, the regression coefficients are calculated from the towing tank tests by researchers of "Architecture navale et systèmes de transports" (ANAST) at the University of Liège (Belgium).

3. Ship maneuvering validations

3.1. Turning circle test

The maneuvering model in section 2.1 is first validated using the standard turning circle test. The ship's parameters are shown in Table 3. The simulation results are plotted in Fig. 4. It can be seen that the trajectory, surge velocity and yaw angle agree well with the experimental data ([5]), which proves the validity of the nonlinear transient hydrodynamic model in this work.

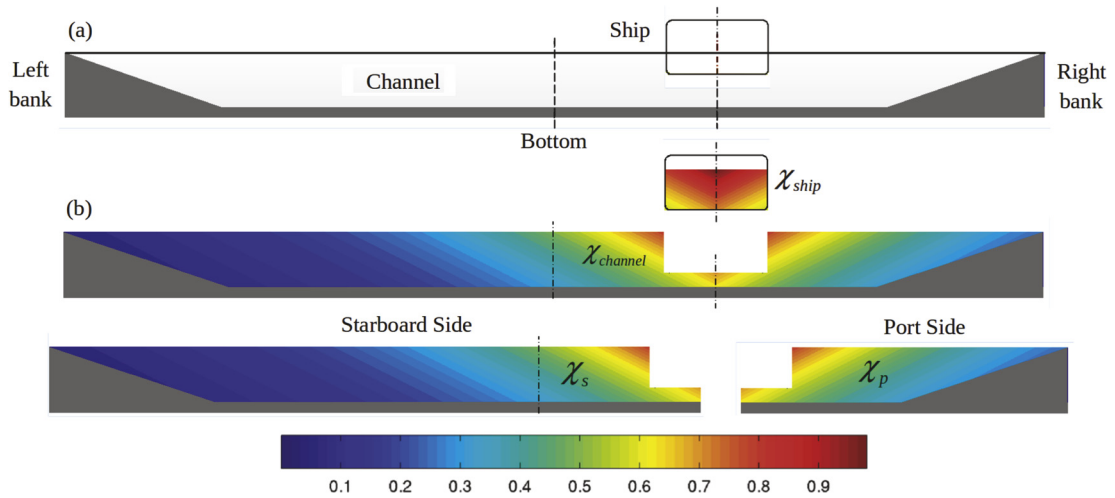


Fig. 3. Weighting coefficient distribution in the confined waterway (cross section). (a) Geometry of the channel; (b) weighting coefficients (equations (25)–(28)).

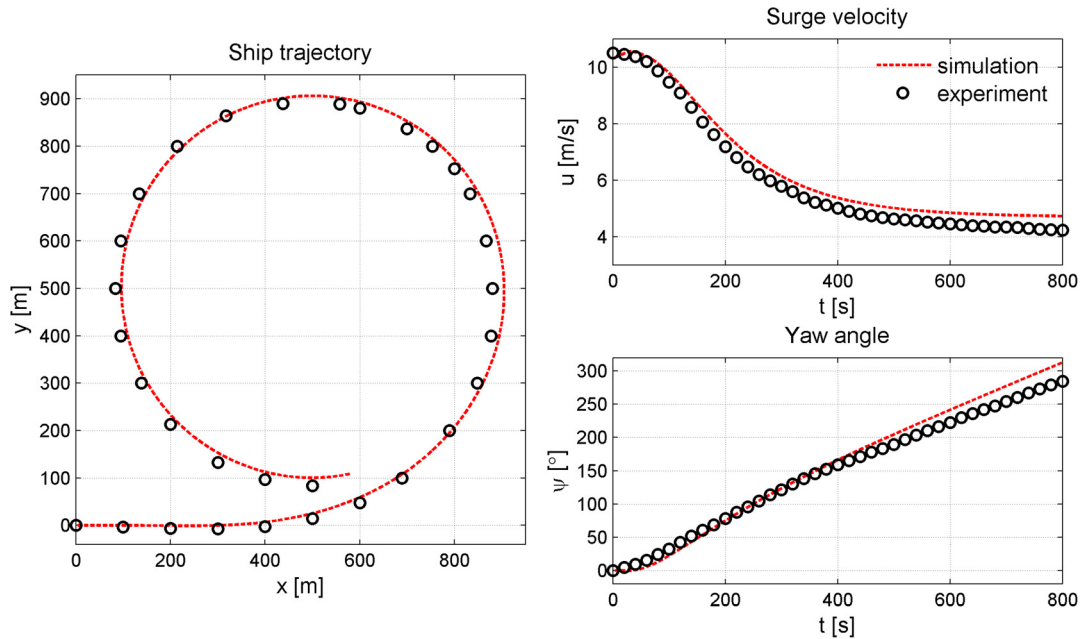


Fig. 4. Results of the turning circle test. The experimental data come from [5].

3.2. Validation of the confinement model

The control parameters of the ship are shown in Table 4. Detailed experimental setups are given in the original paper of Norrbin [13]. The comparison between experimental and simulated results are shown in Fig. 5. The agreement proves the validity and the correct implementation of the confinement model in this study. Because of the adding of the longitudinal force X_B , our results have been greatly improved compared with the work of Du et al. [8]. In the next section, the ship–bank distance and the ship’s speed will be varied to investigate their influences on ship maneuverability.

4. Results and discussions

Three cases are considered in this section, where the separation distance, ship speed, and channel width are varied respectively. The detailed parameters are shown in Table 5. According to the ITTC report [14], when the water depth is less than 1.5 times the ship’s draft, the influence of the channel bottom becomes evident, which is also referred to as the shallow-water effect. In reality, the depth restriction may already be noticed when $h/T < 4$ ([15]). Here, $h/T = 1.38$, which

Table 4
Ship parameters during the validation of the confinement model.

Parameters	Values
δ [°]	0
u_{init} [knots]	5
h [m]	42.64
T [m]	18.46
h/T	2.31
L_b [m]	300
y_s [m]	77.2
y_s/L_{pp}	0.25

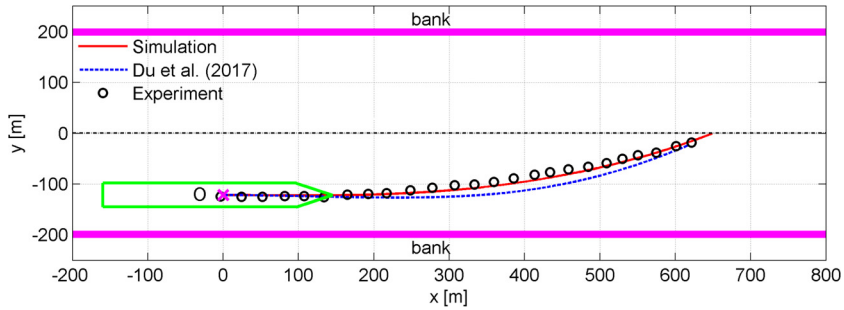


Fig. 5. Validation of the confinement model using the experiments of Norrbin [13] and the work of Du et al. [8].

Table 5
Design of the bank and ship parameters (see Fig. 2).

Parameters	Case 1	Case 2	Case 3
L_p [m]	300	300	100–300
$\tan \alpha$	1:3	1:3	1:3
h [m]	25.5	25.5	25.5
T [m]	18.46	18.46	18.46
y_s [m]	35–80	35	35
u [knots]	8.0	1.0–8.0	8.0
n [rpm]	40	5–40	40
δ [°]	0	0	0

means the designed waterway is in shallow water. The influence distance y_d (Equation (29)) in this study is 274.3 m. So the channel designed in Table 5 is fully confined. The following investigations are carried out under these conditions.

• **Case 1: Influence of the separation distance**

The separation distance refers to the initial distance between the ship and the edge of the channel bottom y_s (see Fig. 2). The ship trajectories and yaw angles are shown in Fig. 6. The ship will first be attracted to the bank by the suction effect. The bow is pushed away by the bank cushion, which can be seen from the increase of the yaw angle. When the repulsion effect induced by the propulsion and the ship–bank interaction exceeds the bank suction, the ship will be pushed away from the bank. When the separation distance is smaller, the bank effect becomes more significant, the ship will be attracted closer to the bank. The bow-out effect is also greater, leading to a larger yaw angle.

The ship trajectories are also compared with the work of Du et al. [8] (Fig. 7), where the case setups are the same, except that the longitudinal force is taken into account in this study. It can be seen that this force will slow down the ship, which further weakens the bank effect.

The minimum distance to the bank is calculated to characterize its relation with the separation distance. By neglecting the curvatures of the ship and assuming the shape is rectangular, the minimum position should lie at the bottom corner at the stern (see Fig. 8). The separation distance y_s is from the midship point to the edge of the channel bottom, which should be converted to the stern. Then

$$y_{sb1} = y_s - \sqrt{(L_{pp}/2)^2 + (B/2)^2} \sin \beta_b \tag{30}$$

where $\beta_b = \psi + \alpha_b$. α_b is determined by the length (L_{pp}) and beam (B) of the ship. ψ is the yaw angle in Fig. 6. Since the bank is tilted, the real minimum distance should be

$$D_{min} = y_{sb1} + y_{sb2} \tag{31}$$

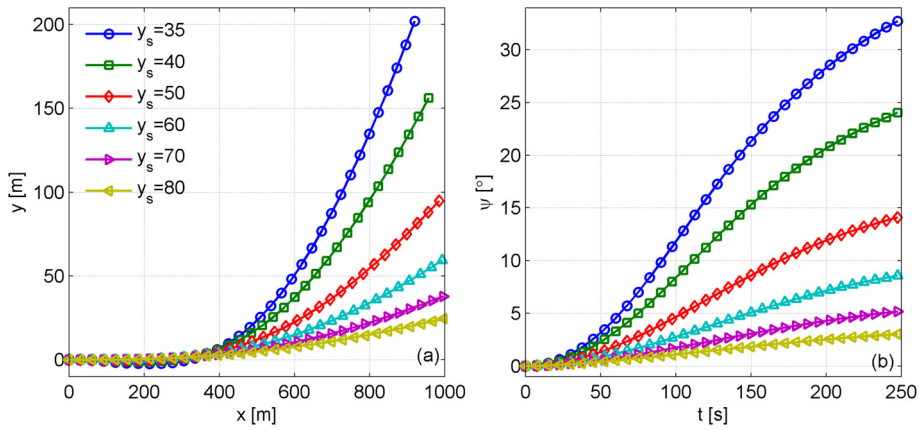


Fig. 6. Ship trajectories (a) and yaw angles (b) at different separation distances.

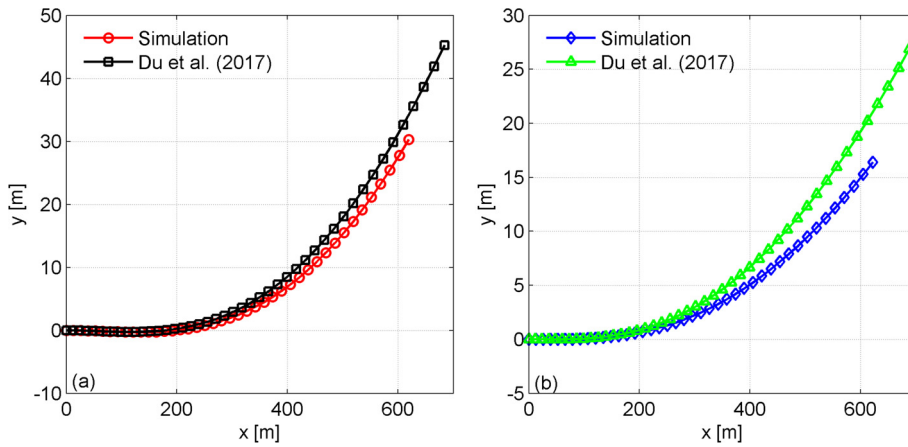


Fig. 7. Ship trajectory comparison with the work of Du et al. [8]. (a) $y_s = 50$ m; (b) $y_s = 75$ m.

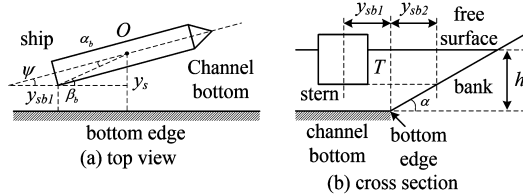


Fig. 8. Sketch for the calculation of the minimum distance to the bank.

where $y_{sb2} = (h - T)/\tan\alpha$. The minimum distance is calculated in Fig. 9. It can be observed that the minimum distance increases with the increase of the separation distance, which corresponds to the real situation. It should be noted that the ship trajectories in Fig. 6 are based on the midship point, which does not take into account the ship’s geometry. As a result, the ship should be maneuvered away from the bank. In the restricted waterway, it is better to steer the ship in the middle of the waterway. To quantitatively characterize the results, a regression equation is obtained based on the data in Fig. 9.

$$D_{\min} = -0.0221y_s^2 + 3.914y_s - 99.98 \quad 0 < y_s < 150 \tag{32}$$

The coefficient of determination (R^2) is 0.9988, indicating a good fitting quality. This equation shows a weak second-order polynomial relation between the minimum distance and the separation distance.

• **Case 2: Influence of the ship’s speed**

Ship speed is varied in order to investigate its influence on ship maneuverability in the restricted waterway. As indicated in Table 5, velocities from 1.0 to 8.0 knots are designed, which cover a wide range in real situations. The ship trajectories and yaw angles are shown in Fig. 10. It can be seen that a lower speed makes the ship experience smaller ship–bank

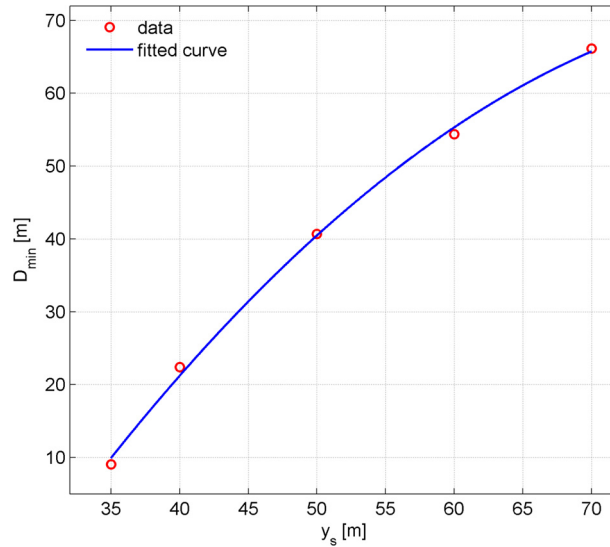


Fig. 9. The minimum distance to the bank as a function of the separation distance.

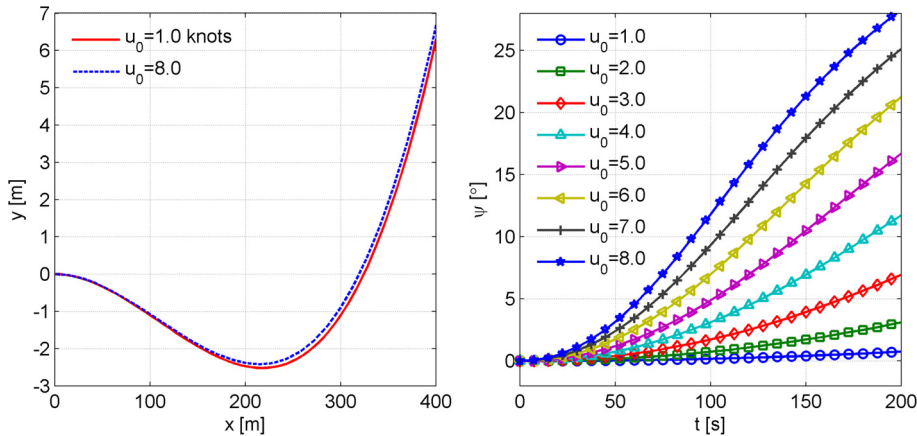


Fig. 10. Ship trajectories (a) and yaw angles (b) at different ship velocities. Only two velocities are presented in (a) for clarity.

interaction, and the deviation from the original trajectory is also smaller. The bow is repelled with a large yaw angle when ship velocity is increased.

The minimum distance to the bank is also calculated to demonstrate its relation with ship speed. The data and fitting curve are shown in Fig. 11. The fitting formula is

$$D_{\min} = 8.638 e^{-0.009u_0} + 0.326 e^{0.148u_0} \quad u_0 > 0 \tag{33}$$

The coefficient of determination (R^2) is 0.999. When its speed is high, the ship will have a large ship–bank interaction. With the bow being repelled, the ship will be propelled away from the bank. So the minimum distance will increase with the increase of ship speed. However, when the ship is fast, ship maneuverability will be changed and the control of the ship will become difficult. Besides, the potential force colliding with the bank will also increase. Therefore, when the ship is navigated near the bank, the minimum distance to the bank and the difficulty of maneuvering should be evaluated to prevent possible accidents.

• **Case 3: Influence of the channel's width**

The influence of the fairway dimension is investigated in this case. The detailed parameters of the ship and fairway can be found in Table 5. The width of the waterway is varied from 100 to 300 m, while the bank slope, the height of the waterway and the water depth are kept the same. The ship is placed with the same separation distance ($y_s = 35$ m) in the waterway, with the initial ship speed 8.0 knots and the rudder angle 0° .

The ship trajectories and yaw angles can be seen in Fig. 12. When the channel width is small, the influences of both banks tend to be symmetric and counteract with each other. The ship's heading will not change intensely and the ship

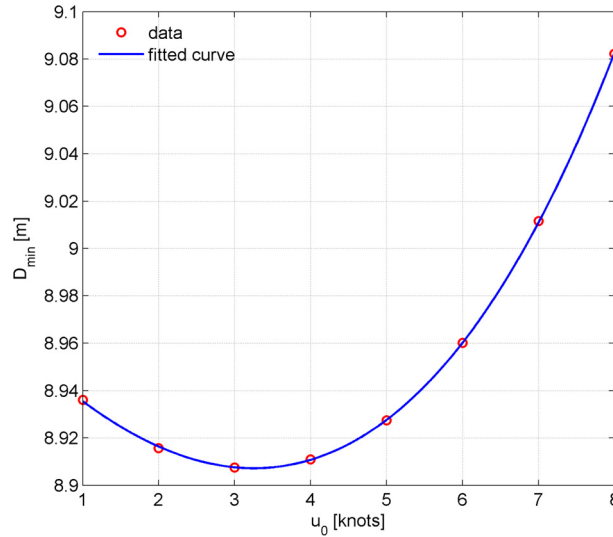


Fig. 11. The minimum distance to the bank as a function of ship velocity.

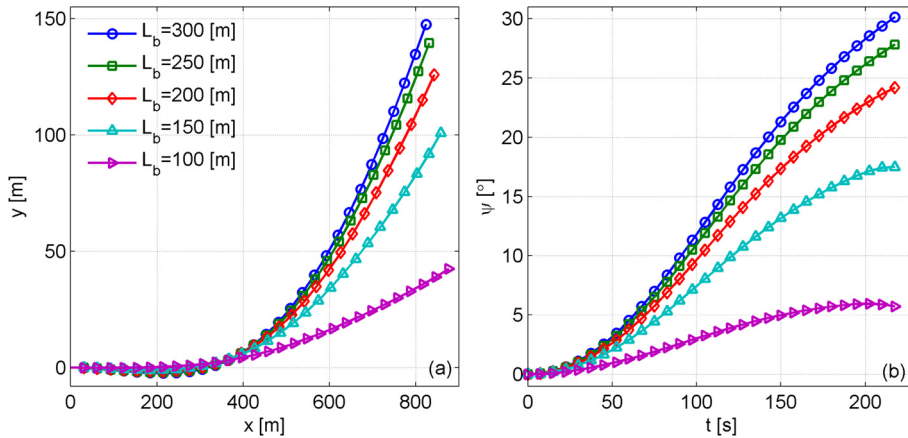


Fig. 12. Ship trajectories (a) and yaw angles (b) at different channel widths.

tends to stick to its original course. Although this is beneficial to the ship's navigation, the maneuvering space in the confined waterway is limited. The confinement of the channel becomes large with a small fairway width, which induces great longitudinal resistance on the ship. As shown in Fig. 13, the ship's advancing speed is dramatically reduced.

The relationship between the minimum ship-bank distance and the channel width is shown in Fig. 14. The minimum distance is observed to decrease with the increase of the channel width. It is noted again that, in this case, the separation distance is fixed, and the channel width is varied. So the asymmetry of the bank effect plays an important role in the appearance of the nearest position between the ship and the bank. The fitting equation is shown below:

$$D_{\min} = 60.52 e^{-0.01446L_b} + 19.42 e^{-0.003L_b} \tag{34}$$

5. Conclusion

In this paper, a model of the confinement effect is implemented in the maneuvering equations, where the confinement effect is considered as additional forces and moment on the ship's hull. The numerical results and the experimental data show good agreement.

Using this method, the ship's maneuverability in the confined waterway is studied with various separation distances, ship speeds and channel widths. The minimum distances to the bank are calculated as functions of the three parameters. Smaller separation distances make the ship deviate more from the original course, and the bow-out effect by the bank cushion is more evident. It is suggested to maneuver the ship away from the bank (in the middle if in a confined waterway), which corresponds to the real case. The influence of ship speed is not so obvious as that of the separation distance. The minimum

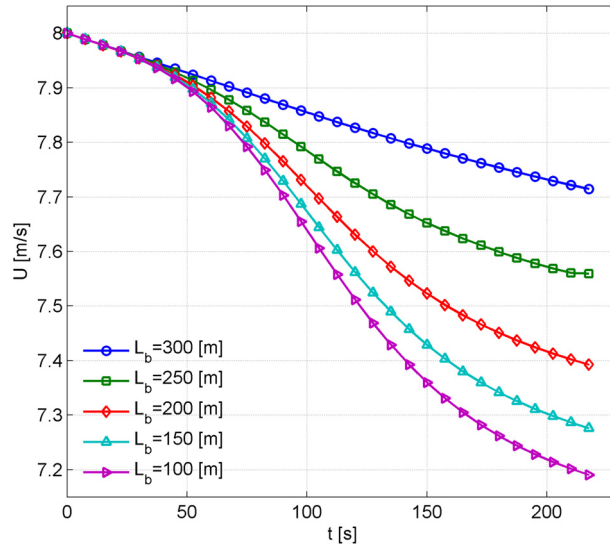


Fig. 13. Ship velocities ($U = \sqrt{u^2 + v^2}$) at different channel widths.

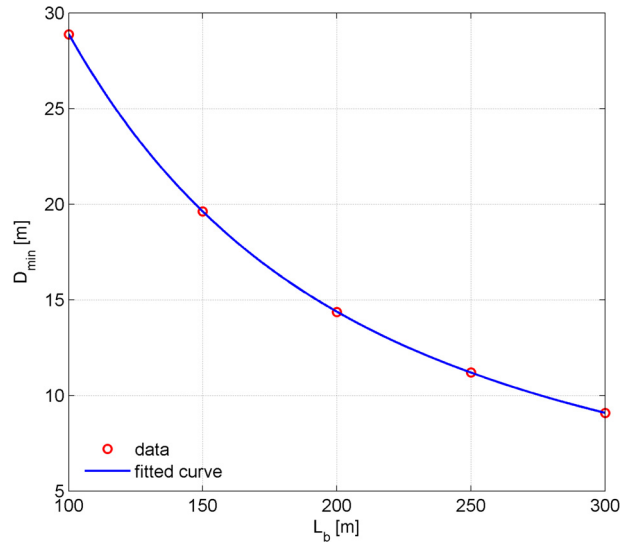


Fig. 14. The minimum distance to the bank as a function of the bank width.

ship–bank distance shows a polynomial relation with ship speed. A smaller channel width is beneficial to maintain the original course since the effects of both banks tend to counteract with each other. However, the confinement will induce large longitudinal resistance on the ship, which greatly reduces the ship’s advancing speed and thus its fuel consumption. Compromises should be made between efficiency and safety. If the efficiency is more significant, a higher speed can be selected, and the ship can be maneuvered in the middle of the waterway. On the contrary, if the safety is more important, the ship can be sailed at a lower speed where ship maneuverability does not change intensively, and even so, these changes can be easily counteracted by the rudder’s action.

Acknowledgements

The first author acknowledges the China Scholarship Council (CSC) for their financial support.

References

[1] S. Bhattacharyya, M. Haddara, Parametric identification for nonlinear ship maneuvering, *J. Ship Res.* 50 (3) (2006) 197–207.
 [2] A.B. Mahfouz, M.R. Haddara, Effect of the damping and excitation on the identification of the hydrodynamic parameters for an underwater robotic vehicle, *Ocean Eng.* 30 (8) (2003) 1005–1025.

- [3] X.-G. Zhang, Z.-J. Zou, Estimation of the hydrodynamic coefficients from captive model test results by using support vector machines, *Ocean Eng.* 73 (2013) 25–31.
- [4] W. Luo, C.G. Soares, Z. Zou, Parameter identification of ship maneuvering model based on support vector machines and particle swarm optimization, *J. Offshore Mech. Arct. Eng.* 138 (3) (2016) 031101.
- [5] K.T. Toan, A. Ouahsine, H. Naceur, K.E. Wassifi, Assessment of ship manoeuvrability by using a coupling between a nonlinear transient manoeuvring model and mathematical programming techniques, *J. Hydrodyn.* 25 (5) (2013) 788–804.
- [6] C.-K. Lee, S.-G. Lee, Investigation of ship maneuvering with hydrodynamic effects between ship and bank, *J. Mech. Sci. Technol.* 22 (6) (2008) 1230–1236.
- [7] C.-K. Lee, Assessment of safe navigation including the effect of ship–ship interaction in restricted waterways, *J. Navig. Port Res.* 27 (3) (2003) 247–252.
- [8] P. Du, A. Ouahsine, K. Toan, P. Sergent, Simulation of ship maneuvering in a confined waterway using a nonlinear model based on optimization techniques, *Ocean Eng.* 142 (2017) 194–203.
- [9] M. Vantorre, Experimental investigation of ship–bank interaction, in: *Proc. International Conference on Marine Simulation and Ship Manoeuvrability (MARSIM'03)*, Kanazawa, Japan, 25–28 August 2003, 2003.
- [10] E. Lataire, Experiment Based Mathematical Modelling of Ship–Bank Interaction, Ph.D. thesis, University of Ghent, Belgium, 2014.
- [11] P.-J. Pompée, About modelling inland vessels resistance and propulsion and interaction vessel–waterway. Key parameters driving restricted/shallow water effects, in: *Proceeding of Smart Rivers*, Buenos Aires, Argentina, 2015.
- [12] S. Geerts, B. Verwerft, M. Vantorre, F. Van Rompuy, Improving the efficiency of small inland vessels, in: *European Inland Waterway Navigation Conference*, Baja, Hungary, 2010.
- [13] N.H. Norrbin, A method for the prediction of the maneuvering lane of a ship in a channel of varying width, in: *Symposium on Aspects of Navigability of Constraint Waterways, including Harbor Entrances*, 1978, pp. 1–16.
- [14] ITTC, The Manoeuvring Committee, Final report and recommendations to the 23rd IEEE International Conference on Information Technology: Coding and Computing (ITCC 2002), Venice, Italy, 2002.
- [15] H. Raven, A computational study of shallow-water effects on ship viscous resistance, in: *29th Symposium on Naval Hydrodynamics*, Gothenburg, Sweden, 2012.